HNBR-Based Dual Network Co-crosslinked Composites with Excellent Tribological Properties under Water Lubrication

Hao Yu , Wuxuan Zheng , Caixia Zhang , Shoubing Chen , Guangke Tian * , Tingmei Wang *

Posted Date: 10 October 2023

doi: 10.20944/preprints202310.0632.v1

Keywords: Co-crosslinking; Tribology; Water lubrication; Rubber

Article

HNBR-Based Dual Network Co-Crosslinked Composites with Excellent Tribological Properties under Water Lubrication

Hao Yu [1,2,3], Wuxuan Zheng [1,2,3], Caixia Zhang [2,3], Shoubing Chen [2,3], Guangke Tian [1,*] and Tingmei Wang [2,3,*]

[1] National Engineering Research Center for Technology and Equipment of Green Coating, Lanzhou Jiaotong University, Lanzhou 730070, PR China; 1449981967@qq.com
[2] Key Laboratory of Science and Technology on Wear and Protection of Materials, Lanzhou Institute of Chemical Physics, Chinese Academy of Sciences, Lanzhou 730000, PR China
[3] Center of Materials Science and Optoelectronics Engineering, University of Chinese Academy of Sciences, Beijing 100049, PR China
* Correspondence: tmwang@licp.cas.cn (T. Wang); tiangke@mail.lzjtu.cn (G. Tian); Tel.: 86-18993053958

Abstract: As one of the important components of underwater propulsion systems, water lubricated bearings are often failure due to mechanical wearing and vibrating, especially under high loads and prolonged friction. In this paper, a dual-network co-crosslinking strategy based on HNBR is proposed, in which the epoxy network connects with the rubber network through Epoxidized Eommia ulmoides gum. The damping, tribological and mechanical properties of the prepared composite are systematically investigated. The results show that this material has excellent friction and vibration damping properties, with a water-lubricated coefficient of friction as low as 0.022 and a wear resistance as high as 3.87 × 10-6mm^3/Nm. Preparing HNBR-based composite by dual network co-crosslinked is proved being a feasible solution to improve the reliability and service life of water-lubricated bearings.

Keywords: co-crosslinking; tribology; water lubrication; rubber

1. Introduction

As an important component of underwater propulsion systems, water-lubricated bearings have attracted much attention in the mechanical field[1-3]. Compared with the traditional oil lubrication method, water-lubricated bearings have many advantages, such as safety, environmental protection, economy and green, thus becoming an important direction of underwater bearing research[4-7]. However, compared with oil lubricated bearings, water-lubricated bearings also have some disadvantages. For example, the poor load carrying capacity and low adsorption capacity of water lead to poor boundary lubrication performance[8-10]. Therefore, it is necessary to further improve the performance of water-lubricated bearings through technical improvement and design optimization, so as to enhance the reliability and service life of water-lubricated bearings and promote their application in non-underwater propulsion systems.

Rubber elastomers, as polymeric water lubrication materials, are effective in reducing bearing friction and wear under water lubrication conditions and have a low coefficient of friction[11-13]. In addition, the rubber material can absorb vibration and shock and reduce the generation of noise and vibration[14]. Among them, hydrogenated nitrile butadiene rubber (HNBR) is a product obtained by catalytic hydrogenation technology of nitrile rubber, which has higher oxidative stability, abrasion resistance, and smaller permanent compression deformation compared with traditional nitrile rubber[15,16].

When HNBR is used alone as a water-lubricated bearing, it generates a lot of heat under higher loads and dry friction conditions, leading to scorching and frictional failure[17]. For this reason,

 doi:10.20944/preprints202310.0632.v1

researchers have conducted numerous studies on HNBR water lubrication materials. Common ways to improve the friction performance include the addition of solid lubricants[18], microcapsules[19], blending[20], and surface modification[21]. Compared with pure HNBR, polymer blending is also a way to improve the performance of rubber materials. Chudzik et al[22]. By adding modified epoxy diene resin to NBR, the addition of 10% unmodified resin (ED-20) resulted in the most significant reduction in friction of NBR vulcanized rubber, with a reduction of 25% in friction. Sang et al[23]. By grafting a silane coupling agent functional layer on the surface of plasma-functionalized polyamide (PA 6), the joining of PA 6 with hydrogenated nitrile butadiene rubber (HNBR) was achieved, and the heat resistance of the material was improved. Zhou et al[3]. investigated the effect of blending different fillers on the friction and wear properties, mechanical properties, and vulcanization properties of HNBR, and the UHMWPE/HNBR composites had the best friction properties with low-speed water lubrication. People are committed to improving the performance of HNBR. Therefore, we believe that the introduction of high-performance polymers with good physicochemical properties can prepare composites with excellent performance.

Eommia ulmoides gum (EUG) is a renewable natural rubber (NR) with excellent dynamic mechanical properties in a wide range of high-performance rubber materials, including tires, vibration-damping devices and acoustic materials[24,25]. Epoxidized Eommia ulmoides gum (EEUG) prepared by simple epoxy functionalization are effective in improving their compatibility with polar ingredients. Wang et al[26]. succeeded in improving the adhesive properties at the Styrene Butadiene Rubber (SBR)/Silicon Dioxide (SiO2) interface with mechanical properties exceeding those of other compatibilizers using epoxy dutasteride rubber as a compatibilizer. Chen et al[27]. developed an EEUG/epoxy (EP) composite coating, where the introduction of EEUG increased the cross-linking density, giving the coating excellent tensile strength and corrosion resistance. Wang et al[28]. prepared a tough biobased composite with a shape memory effect using a dynamic vulcanization technique. Therefore, EEUGs enriched with epoxy groups and double bonds can effectively improve the compatibility of rubbers and polymers such as epoxy resins.

In this study, we propose a dual-network co-crosslinking strategy that combines two networks, rubber and epoxy, to form a homogeneous dual-crosslinked system with multiple phases by introducing epoxidized Eommia ulmoides gum as an intermediate. We investigated the frictional properties of the materials using a ring-block friction and wear tester and revealed the water lubrication mechanism of the dual-network co-crosslinked system. By introducing epoxy Eommia ulmoides gum, we succeeded in linking separate crosslinking systems of rubber and epoxy resin and improving the damping properties of the material. Excitingly, the tribological properties of the material were also significantly improved with the formation of the dual network co-crosslinking system.

2. Materials and Methods

2.1. Materials

Hydrogenated nitrile butadiene rubber, LANXESS 4369, Germany, has an acrylonitrile content of 43% and a Menni viscosity (ML 1 + 4) of 97 at 100°C. Purchased from Meifu New Material Co., Ltd. (Jiangsu). Eommia ulmoides gum (EUG) was obtained from Beijing Huayan Shijia Quality Control Technology Co. Haine epoxy resin was obtained from Wuhan Lanabai Pharmaceutical & Chemical Co. 4,4'-Methylene-bis(2-chloroaniline) (MOCA) was obtained from Anhui Xianglong Chemical Co. Stearic acid, sulfur, zinc oxide, carbon black (N220), tetramethylthiuram disulfide (TMTD), and 2-thiobenzothiazole (MBT) are all industrial grade. All chemicals, unless otherwise stated, may be used without further purification.

 doi:10.20944/preprints202310.0632.v1

2.2. Preparation

2.2.1. Preparation of epoxidized Ecommia ulmoides gum

EUG was dissolved in xylene, hydrogen peroxide and formic acid were mixed at a 1:1 ratio and slowly added to EUG through a constant pressure dropping funnel, and the reaction was carried out at 40°C for 5 hours. At the end of the reaction, an excess of ethanol was added to precipitate and then filtered, washed and dried to obtain eoxidized Ecommia ulmoides gum.

2.2.2. Preparation of HNBR/EEUG composites

HNBR and rubber additives such as zinc oxide, tetramethylthiuram disulfide (TMTD) 2-thiobenzothiazole (MBT), etc. are added to the mixer and mixed well to obtain the rubber masterbatch. The HNBR mother gum was chopped and added to a three-necked flask, and tetrahydrofuran (THF) was added at 1:10, accompanied by stirring for 12 hours to dissolve it completely. EEUG was dissolved in a small amount of THF and subsequently added to the HNBR gum solution along with sulfur and MOCA with stirring for 1 hour. After sufficient stirring, the solvent was removed on a far infrared graphite heating plate at 55°C. The obtained film was alternately triangularly wrapped and rolled 6 times on an open mill. The film was vulcanized in a plate vulcanizer at 150°C and 10 MPa for 30 min. Finally, the samples were cured at 80°C for 3h-120°C 3h-150°C 5h under gradient temperature increase. The mass ratios of the prepared HNBR/EEUG composites HNBR to EEUG were 100:3, 100:5, 100:7, 100:9, and 100:11.

2.2.3. Preparation of dual network co-crosslinked composites

The dual-network co-crosslinked composites were prepared in a similar way to the former preparation method, in which HER and HNBR were dissolved together in THF, and based on the results of the later experiments, the composite of HNBR/EEUG 100:7 was selected as the matrix, and the ratios of HNBR/HER/EEUG were 100:7:3, 100:7:5, 100:7:7, and 100:7:9.

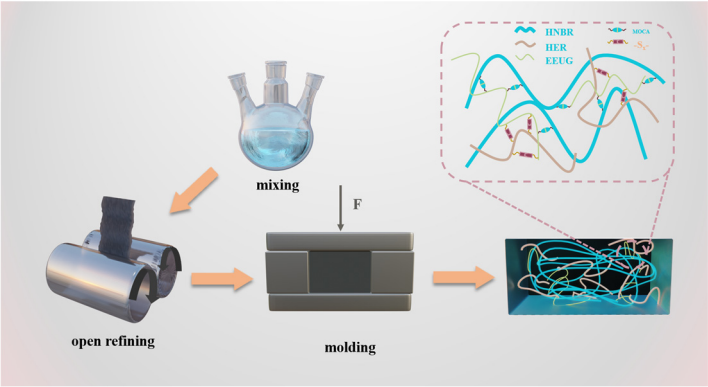

Figure 1. Schematic diagram of the preparation process.

2.3. Tribological tests

Friction wear experiments were carried out using the MRH-3 type ring block wear tester manufactured by Times Test Metals, Inc. under water lubrication conditions, and the friction pair was a tin bronze ring (ZCuSn10Zn2, GB/T 12444-2006). The surface of the specimen ring was ultrasonically cleaned in ethanol by grinding the specimen ring surface with 800 mesh metallographic sandpaper until smooth. At room temperature, the experimental speed was 140 r, the test force was 132 N, and the test drops were added with water on the surface of the friction subsurface. The acceleration rate of all the test drops was 9 ml/min, and the water was refilled at the end of each test. The stable friction value during the last 30 min of the experiment was taken as the average friction coefficient. The surface of the block material was wiped with anhydrous ethanol before and after

Preprints (www.preprints.org) | NOT PEER-REVIEWED | Posted: 10 October 2023 doi:10.20944/preprints202310.0632.v1

friction and dried at 60°C for 2 h. The specific wear rate (Ws, mm^3/Nm) was calculated by the following relation:

$$W_S = V_S/F * 2\pi R * n * nt * t \ (mm^3/Nm) \quad (a)$$

where Vs (mm^3) represents the wear volume of each friction rubber block and is given in the following equation. r denotes the outer diameter of the tin-bronze ring, and F, n, and t represent the normal load (N), rotational speed (rpm), and test time (min), respectively.

$$V_S = \frac{D^2}{8} t \left[2 \sin^{-1} \frac{b}{D} - \sin\left(2 \sin^{-1} \frac{b}{D}\right)\right] \ (mm^3) \quad (b)$$

where D (mm) is the outer diameter of the tin bronze ring and b (mm) and t (mm) are the average width of the abrasion mark and the width of the rubber block, respectively. To ensure the reliability of the experimental data, the average of three measurements is taken as the experimental data.

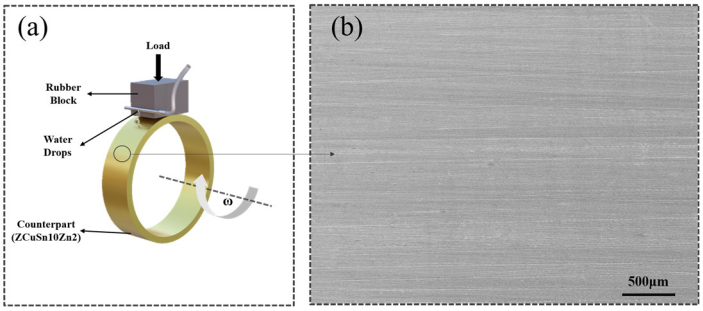

Figure 2. (**a**) Schematic diagram of the friction device (**b**) SEM micrograph of the surface of the paired rings.

2.4. Characterizations

^{1}H NMR spectra were recorded at 25°C on a Bruker AVIII 400 MHz spectrometer. EUG and EEUG were dissolved in CDCl3 and transferred to NMR tubes for subsequent determination. Samples were analyzed using Fourier transform infrared spectroscopy (FT-IR, Bruker S V70). The mechanical properties of the materials were characterized by a universal testing machine (Shimadzu AD-X (5000 N)), and at least three samples were tested to obtain the average value according to the GB/T 528-2009 standard using a tensile rate of 500 mm/min. To clearly observe the micromorphology and analyze the phase behavior of the material, the surface of the material was characterized by AFM atomic force microscopy. The friction surface morphology of the material was observed by SEM, and the friction surface was sprayed with gold to increase the electrical conductivity of the material surface before testing. The contact angle (CA) of water on the surface of a material was measured by the sessile drop method on a DECCA-100 optical contact angle meter (Shenzhen DECCA Precision Instrument Co., Ltd.). To obtain a more accurate value, the CA was measured randomly at three different positions on the friction surface of the sample, and then the arithmetic mean was obtained. The damping properties of the materials were characterized by DMA with the following parameters: the mode was tensile mode, the fixed frequency was 10 Hz, the temperature range was from -60°C to 60°C, and the temperature increase rate was 5°C/min.

3. Results and Discussions

3.1. EEUG characterization

Eucommia ulmoides gum, which is mainly composed of trans-isoprene, is poorly compatible with polar hydrogenated nitrile rubber because of its high degree of crystallinity and nonpolar nature, and epoxy functionalization has become a simple and effective way to improve its compatibility. The successful epoxidation of dulcimer rubber is proved by the FTIR spectra shown in Figure 3(a), which shows that the peak of C=C telescopic vibration at 1665 cm^{-1} decreases after epoxide functionalization, and the symmetric and asymmetric vibrational absorption peaks of C-O-C

Preprints (www.preprints.org) | NOT PEER-REVIEWED | Posted: 10 October 2023 doi:10.20944/preprints202310.0632.v1

symmetrical and asymmetric vibrational absorption peaks are enhanced at 1263 cm^{-1} and 870 cm^{-1}, and 1665 cm^{-1} is C=C telescopic vibration, which decreases the peak after epoxidation, and the peak of C-O-C symmetric and asymmetric telescopic vibrational peaks are observed at 1264 cm-1 and 870 cm^{-1}. In Figure 3(b), the signals at 1.61, 1.98-2.09, and 5.13 ppm are attributed to CH_3, CH_2, and alkene protons, respectively, in the trans-1,4-structure. The peak at 1.29 ppm is attributed to the methyl peak of the epoxide group. The peak at 2.71 ppm is due to the proton resonance of C-O-C, which suggests that some of the double bonds on the EUG chain were successfully epoxidized[29]. Epoxidized Ecommia ulmoides gum has both C=C and epoxy bonds, which can be crosslinked by both MOCA and S at the same time, providing conditions for HNBR to "connect" with HER.

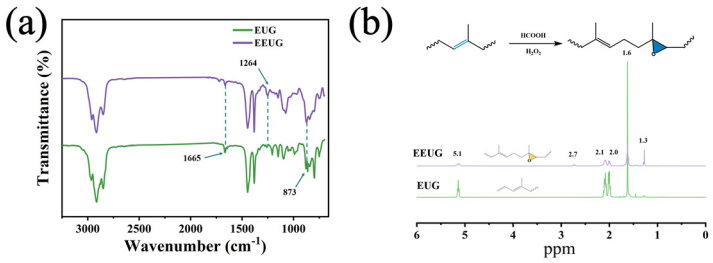

Figure 3. IR image (**a**) and ^1H NMR spectrum (**b**) of EEUG.

3.2. Mechanical Properties of Composite Materials

Mechanical properties have an important impact on the application of materials, and the introduction of EEUG and HER into HNBR will inevitably cause changes in its mechanical properties. For this purpose, tensile measurements were performed, and the results obtained are shown in Figure 4. The tensile strength and elongation at break of the composites increased from 278.52% and 20.41 MPa to 598.4% and 29.4 MPa, respectively, with the addition of EEUG. For rubber composites with different additions of EEUG, the elongation at break and tensile strength increased with the increase of EEUG content. This indicates that the addition of EEUG improves the mechanical properties of pure HNBR. This is due to the good compatibility between EEUG and HNBR, and the incorporation of EEUG as a physical cross-linking point increases the entanglement between molecular chain segments. With the addition of HER, a dual network co-crosslinking system was formed under the dual crosslinking of sulfur and MOCA. The tensile strengths of the materials were all higher than that of the HNBR/EEUG system, with a maximum tensile strength of 36.17 MPa. This is attributed to the incorporation of HER to form a second network, and in the double crosslinking system, the chain segments of the polymers are chemically crosslinked and physically entangled by a combination of chemical cross-linking and physical entanglement, resulting in the formation of a denser structure. The hardness of the material increases at the macroscopic level.

Preprints (www.preprints.org) | NOT PEER-REVIEWED | Posted: 10 October 2023 doi:10.20944/preprints202310.0632.v1

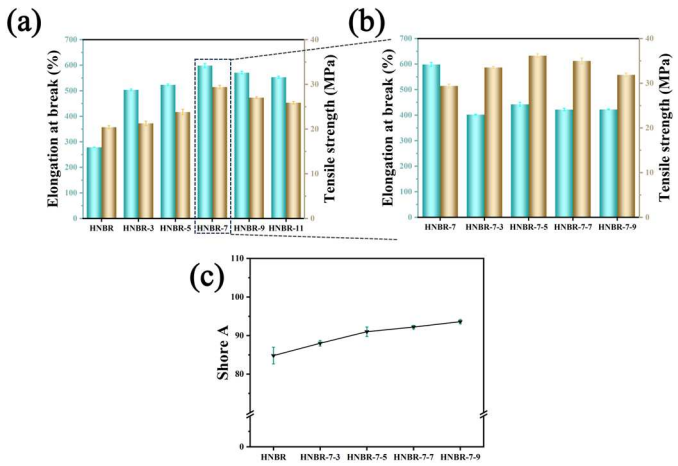

Figure 4. (**a**) Stress–strain diagram of the HNBR/EEUG composite (**b**) Stress–strain diagram of the dual-network co-crosslinked composite (**c**) Shore hardness of the dual-network co-crosslinked composite.

3.3. Damping analysis of composites

Bearings in water lubrication conditions produce severe vibration and are not conducive to the actual service of the material, so the study of the damping properties of composite materials for bearings in vibration damping is of great significance. The damping properties of polymers are closely related to the internal friction generated by the relative slip of the polymer molecular chains[30]. Figure 5 shows the energy storage modulus (E′) and loss factor (Tanδ) versus temperature for different components of HNBR at 10 Hz. With the addition of soft EEUG, the energy storage modulus of the material decreases and is lower than that of the HNBR, but the effective damping range becomes wider. Having the largest energy storage modulus when HNBR/EEUG is 100:7, there is only a single peak in Tanδ for all the samples, which indicates that epoxidation makes a good compatibility between dulcimer rubber and HNBR. With the addition of HER, the energy storage modulus gradually increases, while the loss factor moves toward higher temperatures. This phenomenon may be due to two reasons: one is that the EEUG acts as a "bridge" between HNBR and HER, and the two, through chemical crosslinking to connect the polymer after crosslinking, further reduce the polymer molecular chain of the internal rotation and lead to a further increase in the molecular chain of the internal friction, ultimately accelerating the internal energy dissipation of the polymer. internal energy dissipation, which improves the damping performance of the material; second, it is caused by the larger rigidity brought by the HER five-membered nitrogen heterocycles, so the increase in the HER content leads to the enhancement of the interaction force between the two, which restricts the movement of the molecular chains (chain segments) in the free volume and leads to the increase in Tg. The high HER component leads to the electrostatic repulsive force between the polar groups exceeding the attractive force, resulting in an increase in the intermolecular distance between the molecular chains and a decrease in the glass transition temperature.

Preprints (www.preprints.org) | NOT PEER-REVIEWED | Posted: 10 October 2023 doi:10.20944/preprints202310.0632.v1

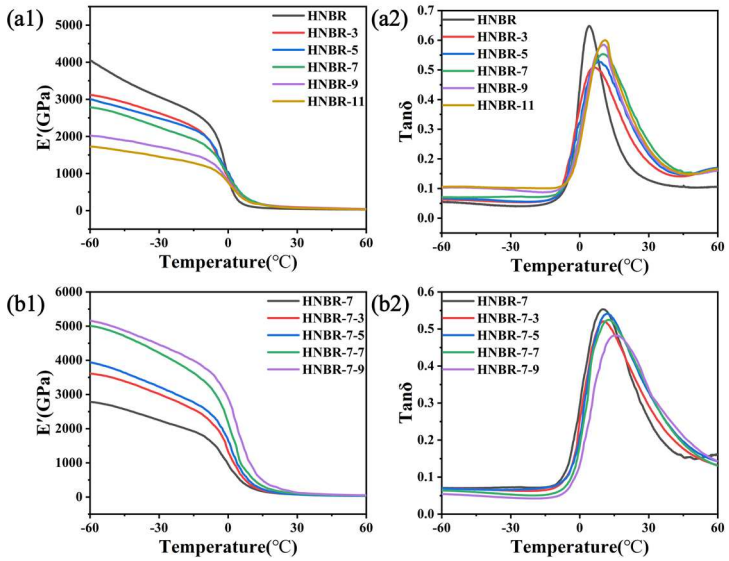

Figure 5. DMA curves of different composites: E' (**a1**) and Tanδ (**a2**) for HNBR/EEUG; E' (**b1**) and Tanδ (**b2**) for HNBR/EEUG/HER.

Table 1. The DMA data of different samples.

HNBR/EEUG	Tanδ_{max}	ΔT (tanδ>0.3)	HNBR/EEUG /HER	tanδ_{max}	ΔT (tanδ>0.3)
100:0	0.65	16.42	100:7	0.55	26.82
100:3	0.51	22.07	100:7:3	0.52	28.45
100:5	0.53	24.95	100:7:5	0.54	30.80
100:7	0.55	26.82	100:7:7	0.52	29.85
100:9	0.58	23.87	100:7:9	0.48	27.24
100:11	0.60	24.08	-	-	-

3.4. Tribological properties of composites

3.4.1. Tribological properties of HNBR/EEUG

The tribological properties of composites have a decisive influence on their service conditions. By investigating the frictional properties of HNBR and EUG at different ratios, the frictional wear curves of HNBR/EEUG composites at different ratios under water lubrication conditions are shown in Figure 6. From Figure 6(a), it can be seen that the friction curves showed very different trends after the addition of EEUG. The HNBR showed an increasing and then decreasing trend at the beginning of the friction, while the friction coefficients all showed a rapid decrease after the addition of EEUG, and then they all leveled off. This is because the pure HNBR in the early friction, due to the growth of the transfer film friction vice contact area presents a boundary lubrication state, with the growth of the transfer film leading to the friction coefficient first increasing and then decreasing. HNBR/EEUG composites slide early, and the formation of a water film makes the material friction coefficient decrease rapidly from the boundary lubrication transition to the mixed lubrication. With water film stabilization, the friction coefficient of the decline gradually slows down and eventually stabilizes. With the increase in EEUG content, the friction coefficient appeared to decrease and then increase. At 7%, the material's coefficient of friction reached a minimum of 0.047, and it is exciting that the friction coefficient of the addition of EEUG is less than that of the pure HNBR. It can be concluded that the addition of EEUG is of great significance in improving the tribological properties of HNBR. The reduction in the friction coefficient is mainly attributed to the plasticizing and softening effect of EEUG on HNBR, which makes the contact area between the friction pair increase, and the larger friction surface makes the water film have a larger carrying capacity[31]. With the addition of EEUG, the wear rate increases gradually, and the reduction in hardness makes it easier

Preprints (www.preprints.org) | NOT PEER-REVIEWED | Posted: 10 October 2023 doi:10.20944/preprints202310.0632.v1

for the material to adhere to the surface of the pair under shear, which reduces the load-bearing capacity of the water film breakage, increases the coefficient of friction, and makes it easier to wear[32].

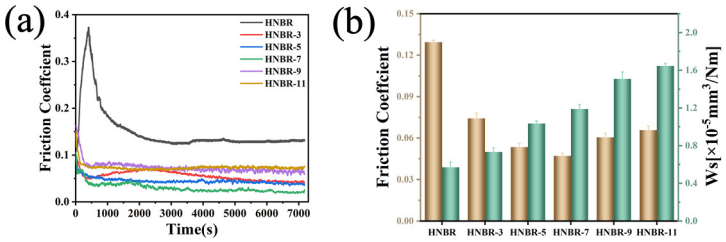

Figure 6. (**a**) Friction profile coefficients (**b**) Average COF and Ws of HNBR/EEUG with different blending ratios.

To study the microscopic wear of the friction material, a scanning electron microscope was used to observe the friction surface. As shown in Figure 7(a), the pure HNBR friction surface has stripping and microcracks along the friction direction, which is mainly dominated by adhesive wear. Figure 7(b~f) After the addition of EEUG, the friction surface shows plow furrows, which are mainly dominated by abrasive wear, which is caused by the microcutting of the polymer by the hard tin-bronze surface. With the addition of EEUG, the modulus of the material gradually decreases, which reduces the abrasion resistance of HNBR and aggravates the abrasion of the material under strong shear force.

The results show that the incorporation of EEUG effectively improves the friction properties under water lubrication conditions, and the coefficient of friction of the composites decreases by nearly two thirds relative to that of pure HNBR at an EEUG content of 7%, but the incorporation of EEUG reduces the wear resistance of pure HNBR. Therefore, we propose a dual-network co-crosslinking system based on the addition of HNBR/EEUG 100:7 with the addition of polar HER and expect these dual-network co-crosslinked composites to have excellent tribological properties.

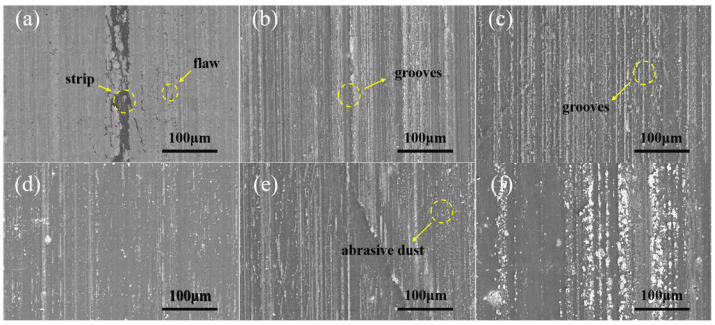

Figure 7. (**a**) SEM micrographs of the wear surfaces of pure HNBR and different HNBR/EEUG ratios: (**b**) 100:3, (**c**) 100:5, (**d**) 100:7, (**e**) 100:9, and (**f**) 100:11.

3.4.2. Frictional properties of dual network co-crosslinked composites

The curves of the friction coefficients of different dual network co-crosslinked systems as a function of test time and the effect of HER content on the average friction coefficients and wear rates of the dual network co-crosslinked systems are shown in Figure 8. Figure 8(a) shows images of the friction coefficient with time for dual network co-crosslinked systems with different HER contents. In the early stage of friction, with the addition of HER content, the friction time during friction is gradually shortened, and the fluctuation of the friction coefficient decreases due to the better damping property of the material. The friction coefficient decreases rapidly and stabilizes, which is attributed to the uniform multiphase structure of the matrix material, and the friction coefficient decreases to 0.022. With the addition of HER to form a double network cocrosslinking system, the hardness and modulus of the material gradually increased, greatly improving the wear resistance of

Preprints (www.preprints.org) | NOT PEER-REVIEWED | Posted: 10 October 2023 doi:10.20944/preprints202310.0632.v1

the material. The coefficient of friction is reduced, and at the same time, there is a better improvement in the wear resistance, and the wear rate is reduced to 3.87×10-6mm³/Nm. The enhanced friction performance is mainly attributed to the following two aspects. First, the synergistic effect of HER incorporation into the gradually formed dual network enables the water lubrication process from boundary lubrication to mixing lubrication quickly, resulting in smaller fluctuations in the material friction coefficient. Second, the gradual formation of the second network leads to a gradual increase in the modulus and hardness of the composite material, smaller plastic deformation makes the material more resistant to shear, and the boundary lubrication performance of the material gradually increases, making the material more wear-resistant.

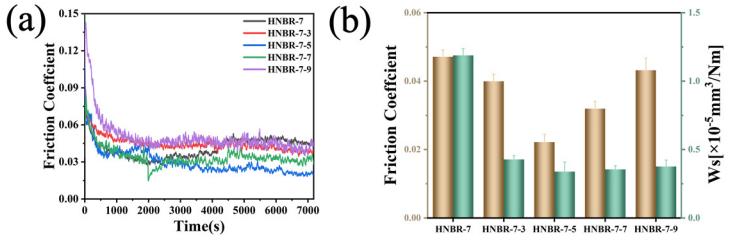

Figure 8. (**a**) Friction profile coefficients and (**b**) average COF and Ws for double network co-crosslinked composites at different ratios.

Figure 9 shows SEM images of the friction surfaces of the dual network co-crosslinked composites at different mass ratios. As shown in Figure 9 (b, c, d), a small amount of grooves gradually disappeared after the formation of the dual network co-crosslinking system, and the friction surface became flatter, mainly dominated by slight plastic deformation. The flat friction surface makes the water film stronger and more complete, which is more conducive to the separation of the water film from the friction sub-surface, while the material friction surface produces only a small amount of abrasive debris[33]. As Figure 9(c) shows, the friction surface is flat with only a small amount of abrasive debris, which is mainly dominated by slight abrasive wear[34]. All the above results indicate that the dual-network co-crosslinked composites possess a low coefficient of friction and wear rate.

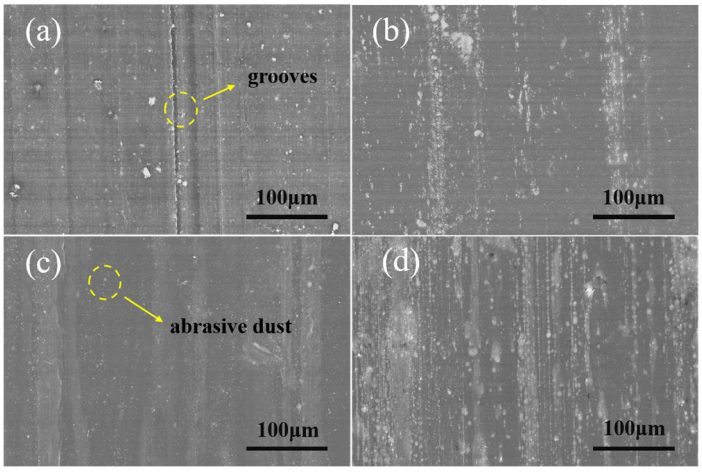

Figure 9. SEM micrographs of worn surfaces of different ratios of double network co-crosslinked composites: (**a**) 100:7:3, (**b**) 100:7:5, (**c**) 100:7:7, and (**d**) 100:7:9.

3.5. Microscopic morphology analysis

The phase morphology of the friction surface was examined using AFM in tap mode. The surface roughness and surface properties of the composite material are critical for the friction properties of the material. The AFM image is 256×256 pixels with a scanning range of 5 μm×5 μm. The AFM image of the material is shown in Figure 10. From the comparison of the AFM morphology of the friction

Preprints (www.preprints.org) | NOT PEER-REVIEWED | Posted: 10 October 2023 doi:10.20944/preprints202310.0632.v1

surface after friction with the phase image, Figures a1~c1 show that in the material surface images, the material rms roughness Rq is 9.85 nm, 8.01 nm and 7.92 nm in order, and the roughness decreases in order, which corresponds to the friction coefficient of the material[35]. The smoother surface may be an important factor in the formation of a stable water film during the friction process, avoiding large protrusions that can pierce the water film and weaken the lubrication effect. The low roughness reduces the mutual resistance between the friction partners and thus improves the boundary lubrication, resulting in a material with a lower coefficient of friction and wear rate[36]. The corresponding phase diagrams show that the latter has changed considerably from pure HNBR, as shown in Figure a2, where agglomeration of carbon black particles is unavoidable in pure HNBR, and the addition of EEUG improves the compatibility of carbon black. No obvious phase separation was observed in the phase diagrams of the latter two, which proves that the components of the prepared materials have good compatibility.

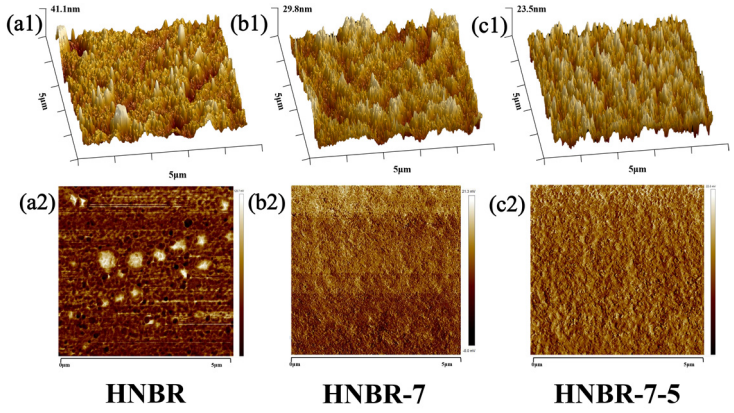

Figure 10. AFM micrographs and phase diagrams of the samples.

3.6. Water contact angle

The water contact angle was tested on the friction surface of the samples. As shown in Figure 11, the water contact angle decreases sequentially, and the water contact angle of the dual network co-crosslinked system decreases by 22.8° with respect to the pure HNBR. The hydrophilicity of the material improves due to the introduction of both EEUG and HER with hydrophilic groups[37]. The hydrophilic surface facilitates the formation of a water film during friction, which can better separate the friction partners, thus reducing the coefficient of friction and wear rate.

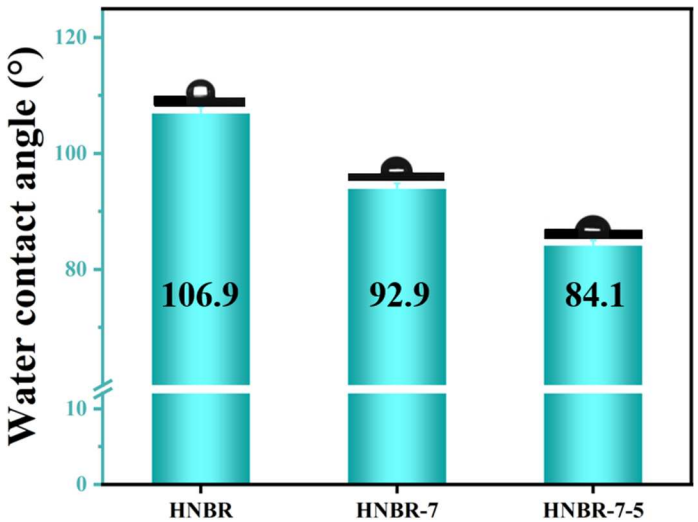

Figure 11. Water contact angle images of samples.

Preprints (www.preprints.org) | NOT PEER-REVIEWED | Posted: 10 October 2023 doi:10.20944/preprints202310.0632.v1

3.7. Long-term wear test

To understand the wear resistance of rubber matrix composites co-crosslinked with dual networks, long-term friction and wear experiments were carried out, and the experimental conditions were set at a 132 N load and 140 rpm, and the experimental time was 12 hours. As shown in Figure 12(a), the double-network co-crosslinked rubber matrix composites have smoother and lower friction coefficients under prolonged friction, and the SEM friction surface images are shown in Figure 12(b, c, and d). HNBR-7-5 has the smoothest and flatest friction surface, which is direct proof of the material's good abrasion resistance. Overall, HNBR-7-5 still has good tribological properties after the long-term wear test.

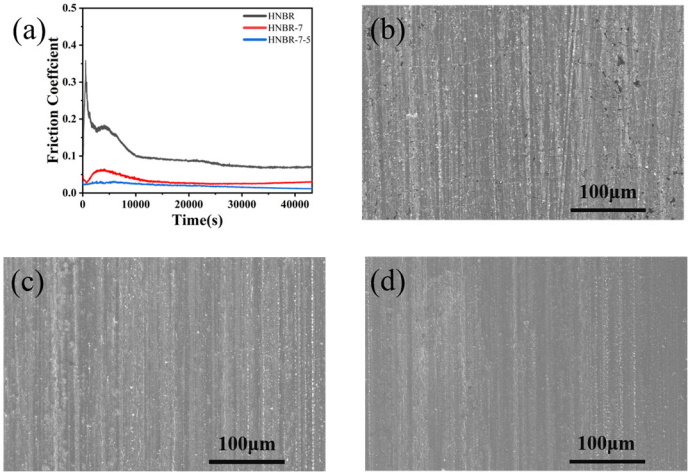

Figure 12. Comparison of friction curves for different samples along 12 h (**a**) and the after-wear surface micrograph for sample, HNBR(**b**), HNBR-7(**c**) and HNBR-7-5 (**d**).

4. Conclusions

In this paper, a dual-network co-crosslinked rubber matrix composite is developed. By using epoxidized Eommia ulmoides gum as a "bridge" between HNBR and HER, the two are chemically cross-linked. Then, the mechanical properties, damping properties, friction properties under water lubrication conditions and microscopic morphology of the composites were systematically investigated. Atomic force microscopy results show that the dual-network co-crosslinked composites have a uniform phase morphology and a flatter friction surface, friction properties and damping properties. The frictional properties of the dual-network co-crosslinked composites were significantly improved with the formation of dual networks, the friction coefficients of COF and Ws were reduced to 0.022, and the wear rate was reduced to 3.87 × 10-6mm^3/Nm in HNBR/EEUG/HER 100:7:5. The effective damping temperature domain of the composites is increased by 87.6% compared with that of pure HNBR. New ideas and practices are provided for the design of composites with good water lubrication and vibration damping properties in the field of underwater propulsion.

Author Contributions: Conceptualization, H.Y., G.T. and T.W.; methodology, S.C.; validation, C.Z., W.Z.; investigation, S.C.; writing—original draft preparation, H.Y.; writing—review and editing, G.T.; visualization, W.Z.; supervision, T.W.; project administration, G.T.; funding acquisition, T.W. All authors have read and agreed to the published version of the manuscript.

Acknowledgments: Supported by the Strategic Priority Research Program of the Chinese Academy of Sciences (NO. XDB0470102).

Conflicts of Interest: The authors declare no conflict of interest.

References

1. Wang, J.; Yan, F.; Xue, Q. Tribological behaviors of some polymeric materials in sea water. *Science Bulletin* **2009**, *54*, 4541-4548, doi:10.1007/s11434-009-0578-4.
2. Litwin, W. Experimental research on water lubricated three layer sliding bearing with lubrication grooves in the upper part of the bush and its comparison with a rubber bearing. *Tribology International* **2015**, *82*, 153-161, doi:10.1016/j.triboint.2014.10.002.
3. Zhou, G.; Wu, K.; Pu, W.; Li, P.; Han, Y. Tribological modification of hydrogenated nitrile rubber nanocomposites for water-lubricated bearing of ship stern shaft. *Wear* **2022**, *504-505*, doi:10.1016/j.wear.2022.204432.
4. Masuko, M.; Suzuki, A.; Sagae, Y.; Tokoro, M.; Yamamoto, K. Friction characteristics of inorganic or organic thin coatings on solid surfaces under water lubrication. *Tribology International* **2006**, *39*, 1601-1608, doi:10.1016/j.triboint.2006.03.002.
5. Yamamoto, K.; Matsukado, K. Effect of hydrogenated DLC coating hardness on the tribological properties under water lubrication. *Tribology International* **2006**, *39*, 1609-1614, doi:10.1016/j.triboint.2006.01.004.
6. Mou, Z.; Yan, R.; Peng, J.; Li, Y.; Huang, Z.; Wang, Z.; Zhao, B.; Xiao, D. Synthesis of polyzwitterionic carbon dots with superior friction and fatigue control behaviors under water lubrication. *Chemical Engineering Journal* **2023**, *465*, doi:10.1016/j.cej.2023.142986.
7. Vadivel, H.S.; Golchin, A.; Emami, N. Tribological behaviour of carbon filled hybrid UHMWPE composites in water. *Tribology International* **2018**, *124*, 169-177, doi:10.1016/j.triboint.2018.04.001.
8. Liu, S.; Luo, J.; Li, G.; Zhang, C.; Lu, X. Effect of surface physicochemical properties on the lubricating properties of water film. *Applied Surface Science* **2008**, *254*, 7137-7142, doi:10.1016/j.apsusc.2008.05.319.
9. Wu, Z.; Guo, Z.; Yuan, C. Influence of polyethylene wax on wear resistance for polyurethane composite material under low speed water-lubricated conditions. *Wear* **2019**, *426-427*, 1008-1017, doi:10.1016/j.wear.2018.11.034.
10. Wang, Q.; Zhou, F. Progress in Tribological Properties of Nano-Composite Hard Coatings under Water Lubrication. *Lubricants* **2017**, *5*, doi:10.3390/lubricants5010005.
11. Qu, C.; Zhang, N.; Wang, C.; Wang, T.; Wang, Q.; Li, S.; Chen, S. MoS2/CF synergistic reinforcement on tribological properties of NBR/PU/EP interpenetrating polymer networks. *Tribology International* **2022**, *167*, doi:10.1016/j.triboint.2021.107384.
12. Zang, L.; Chen, D.; Cai, Z.; Peng, J.; Zhu, M. Preparation and damping properties of an organic–inorganic hybrid material based on nitrile rubber. *Composites Part B: Engineering* **2018**, *137*, 217-224, doi:10.1016/j.compositesb.2016.11.038.
13. Zhou, Y.-J.; Wang, D.-G.; Guo, Y.-B. The Reduction of Static Friction of Rubber Contact under Sea Water Droplet Lubrication. *Lubricants* **2017**, *5*, doi:10.3390/lubricants5020012.
14. Litwin, W. Properties comparison of rubber and three layer PTFE-NBR-bronze water lubricated bearings with lubricating grooves along entire bush circumference based on experimental tests. *Tribology International* **2015**, *90*, 404-411, doi:10.1016/j.triboint.2015.03.039.
15. Narynbek Ulu, K.; Huneau, B.; Verron, E.; Béranger, A.S.; Heuillet, P. Effects of acrylonitrile content and hydrogenation on fatigue behaviour of HNBR. *Fatigue & Fracture of Engineering Materials & Structures* **2019**, *42*, 1578-1594, doi:10.1111/ffe.12974.
16. Yeo, Y.-G.; Park, H.-H.; Lee, C.-S. A study on the characteristics of a rubber blend of fluorocarbon rubber and hydrogenated nitrile rubber. *Journal of Industrial and Engineering Chemistry* **2013**, *19*, 1540-1548, doi:10.1016/j.jiec.2013.01.021.
17. Dong, C.; Shi, L.; Li, L.; Bai, X.; Yuan, C.; Tian, Y. Stick-slip behaviours of water lubrication polymer materials under low speed conditions. *Tribology International* **2017**, *106*, 55-61, doi:10.1016/j.triboint.2016.10.027.
18. Yang, W.; Wang, C.; Liu, Z.; Tan, J. Curing, mechanical, and tribological properties of hydrogenated nitrile butadiene rubber reinforced with Al_2O_3 nanoparticles. *Polymer Composites* **2022**, *43*, 4588-4599, doi:10.1002/pc.26714.
19. Zhang, L.; Xie, G.; Wu, S.; Peng, S.; Zhang, X.; Guo, D.; Wen, S.; Luo, J. Ultralow friction polymer composites incorporated with monodispersed oil microcapsules. *Friction* **2019**, *9*, 29-40, doi:10.1007/s40544-019-0312-4.
20. Zhang, J.; Wang, L.; Zhao, Y. Understanding interpenetrating-polymer-network-like porous nitrile butadiene rubber hybrids by their long-period miscibility. *Materials & Design* **2013**, *51*, 648-657, doi:10.1016/j.matdes.2013.04.073.

21. Liu, Y.; Shuai, C.; Lu, G.; Yang, X.; Hu, X. Preparation of polyethylene glycol brush grafted from the surface of nitrile butadiene rubber with excellent tribological performance under aqueous lubrication. *Materials & Design* **2022**, *224*, doi:10.1016/j.matdes.2022.111310.
22. Chudzik, J.; Bielinski, D.M.; Demchuk, Y.; Bratychak, M.; Astakhova, O. Influence of Modified Epoxy Dian Resin on Properties of Nitrile-Butadiene Rubber (NBR). *Materials (Basel)* **2022**, *15*, doi:10.3390/ma15082766.
23. Sang, J.; Sato, R.; Aisawa, S.; Hirahara, H.; Mori, K. Hybrid joining of polyamide and hydrogenated acrylonitrile butadiene rubber through heat-resistant functional layer of silane coupling agent. *Applied Surface Science* **2017**, *412*, 121-130, doi:10.1016/j.apsusc.2017.03.254.
24. Yang, F.; Dai, L.; Liu, T.; Zhou, J.; Fang, Q. Preparation of high-damping soft elastomer based on Eucommia ulmoides gum. *Polymer Bulletin* **2019**, *77*, 33-47, doi:10.1007/s00289-019-02723-0.
25. Dong, M.; Zhang, T.; Zhang, J.; Hou, G.; Yu, M.; Liu, L. Mechanism analysis of Eucommia ulmoides gum reducing the rolling resistance and the application study in green tires. *Polymer Testing* **2020**, *87*, doi:10.1016/j.polymertesting.2020.106539.
26. Wang, Y.; Liu, J.; Xia, L.; Shen, M.; Xin, Z.; Kim, J. Role of epoxidized natural Eucommia ulmoides gum in modifying the interface of styrene-butadiene rubber/silica composites. *Polymers for Advanced Technologies* **2019**, *30*, 2968-2976, doi:10.1002/pat.4726.
27. Chen, B.; Wu, Q.; Li, J.; Lin, K.; Chen, D.; Zhou, C.; Wu, T.; Luo, X.; Liu, Y. A novel and green method to synthesize a epoxidized biomass eucommia gum as the nanofiller in the epoxy composite coating with excellent anticorrosive performance. *Chemical Engineering Journal* **2020**, *379*, doi:10.1016/j.cej.2019.122323.
28. Wang, Y.; Liu, J.; Xia, L.; Shen, M.; Xin, Z. Super-tough poly(lactic acid) thermoplastic vulcanizates with heat triggered shape memory behaviors based on modified natural Eucommia ulmoides gum. *Polymer Testing* **2019**, *80*, doi:10.1016/j.polymertesting.2019.106077.
29. Yue, P.-P.; Rao, J.; Leng, Z.-J.; Chen, G.-G.; Hao, X.; Peng, P.; Peng, F. An electrospun composite of epoxidized Eucommia ulmoides gum and SiO2-GO with ultraviolet resistance. *Journal of Materials Science* **2022**, *57*, 4862-4875, doi:10.1007/s10853-022-06908-3.
30. Qu, C.; Wang, T.; Wang, Q.; Chen, S. A novel ternary interpenetrating polymer networks based on NBR/PU/EP with outstanding damping and tribological properties for water-lubricated bearings. *Tribology International* **2022**, *167*, doi:10.1016/j.triboint.2021.107249.
31. Yu, P.; Li, G.; Zhang, L.; Zhao, F.; Guo, Y.; Pei, X.-Q.; Zhang, G. Role of SiC submicron-particles on tribofilm growth at water-lubricated interface of polyurethane/epoxy interpenetrating network (PU/EP IPN) composites and steel. *Tribology International* **2021**, *153*, doi:10.1016/j.triboint.2020.106611.
32. Fukahori, Y.; Gabriel, P.; Liang, H.; Busfield, J.J.C. A new generalized philosophy and theory for rubber friction and wear. *Wear* **2020**, *446-447*, doi:10.1016/j.wear.2019.203166.
33. Yin, T.; Wei, D.; Wang, T.; Xie, Z. Thermal compression and accumulation effect on lubrication regime transition mechanism of water seal. *Tribology International* **2023**, *181*, doi:10.1016/j.triboint.2023.108285.
34. Hale, J.; Lewis, R.; Carré, M.J. Rubber friction and the effect of shape. *Tribology International* **2020**, *141*, doi:10.1016/j.triboint.2019.105911.
35. Bai, C.; Qiang, L.; Zhang, B.; Gao, K.; Zhang, J. Optimizing the tribological performance of DLC-coated NBR rubber: The role of hydrogen in films. *Friction* **2021**, *10*, 866-877, doi:10.1007/s40544-021-0498-0.
36. Emami, A.; Khaleghian, S.; Taheri, S. Asperity-based modification on theory of contact mechanics and rubber friction for self-affine fractal surfaces. *Friction* **2021**, *9*, 1707-1725, doi:10.1007/s40544-021-0485-5.